Animation of Facial Expressions by Physical Modeling

Yu Zhang†, Edmond C. Prakash†† and Eric Sung†

†School of Electrical and Electronic Engineering,††School of Computer Engineering
Nanyang Technological University, Singapore

Abstract

In this paper, we propose a physically-based 3D dynamic facial model based on anatomical knowledge for realistic facial expression animation. The facial model incorporates a physically-based approximation to facial skin tissue and a set of anatomically-motivated facial muscle actuators. The tissue model has multilayered mass-spring structure which approximates different types of facial tissue. Two kinds of biphasic springs, structural springs and shear springs, are included in our model to simulate nonlinear elastic behavior of the skin. Facial muscle models are presented to emulate facial muscle contraction. In the muscle model, two factors, the muscle force scaling factor and muscle strength factor provide us macro and micro control of the muscle influence respectively. Based on the facial anatomy, these contractile muscles are inserted at anatomically correct position within the dynamic skin model. Lagrangian mechanics governs the dynamics, dictating the deformation of facial surface in response to muscle forces. The dynamic facial animation algorithm runs at interactive rate with continuous 3D display on a graphics workstation.

1. Introduction

For years, realistic facial expression animation has been one of the most fundamental problems in computer graphics and one of the most difficult. Indeed, attempts to model and animate realistic human faces date back to the early 70's, with significant effort devoted to this field since then. In recent years, facial animation has been used in such diverse areas as character animation in entertainment industry and advertising, model-based video coding, man-machine interface agents and avatars, facial expression recognition and facial surgery planning. However, the task of accurately modeling the expressive human face by computer remains a major challenge. There are several factors that make realistic facial expression modeling so elusive. First, the representation of the face itself. The human face is an extremely complex geometric form. For example, the human face model used in Pixar's Toy Story[14] had several thousand control points each. Moreover, the face exhibits countless tiny creases and wrinkles, as well as subtle variation in color and texture — all of which are crucial for our comprehension and appreciation of facial expressions. Second, the modeling of motion. Since facial movement is a product of the underlying skeletal and muscular forms, as well as the mechanical properties of the skin and subcutaneous layers (which vary in thickness and composition in different parts of the face). This is very complex, because there are numerous specific muscles and important interactions between muscles and bone structure. All of those problems are enormously magnified by the fact that we, as humans, have an uncanny ability to read expressions — an ability that is not merely a learned skill, but is part of our deep-rooted instincts. For facial expressions, the slightest deviation from truth is something any person will immediately detect.

Researchers have devoted significant efforts to the modeling and deformation of the human face shape. In the literature, most facial animation approaches were based on the surface model from standard polygonal surface meshes[1, 2, 4, 15, 16, 17] to parametric surfaces such as B-spline[13] and hierarchical B-spline[22]. Surface model is conceptually simple, providing ease of control and rapid computation. But it has litter relation to physical reality of a layered skin tissue, and therefore tend to lack realism. Since the overall appearance of a human face is very much influenced by its internal tissue and muscle structure, the multilayered model is the most promising for realistic facial animation. The multilayered model should contain different types of facial tissue and model the interactions between them. The key advantage of layered methodology is that once the layered structure is es-

tablished, only the underlying muscle need to be scripted for animation; expressive skin deformations are generated automatically.

Our goal is to achieve a realistic human facial expression animation using physically-based modeling approach from the anatomical perspective and in an acceptable time for interactive applications. In this study, we propose a 3D face model which incorporates a physically-based approximation to facial skin tissue and a set of anatomically-motivated facial muscle actuators. The mechanism of generating facial expressions with our model is very close to the actual one in the human face. Three kinds of muscle models are presented to simulate facial muscles contraction. In the muscle model, two factors, the muscle force scaling factor and muscle strength factor provide macro and micro control of the muscle influence respectively. The biomechanical facial tissue model is constructed by a multilayered elastic mass-spring meshes. Two kinds of biphasic springs, structural springs and shear springs, are included in the model to simulate the nonlinear elastic behavior of the skin. To synthesize facial expressions, we make an important hypothesis about it, namely, that any facial expression can be viewed as a weighted linear combination of the contraction of a set of typical facial muscles. When muscles contract, by solving the dynamic equation for each skin node, the flexible and realistic facial expressions can be animated in real-time.

1.1. Related Work

Previous studies for facial modeling and animation started with the seminal work of Parke[15]. He used a combination of digitized expressions and linear interpolation of features such as eyelids, eyebrows and jaw-rotation. Facial motions are described as a pair of numeric tuples which identify the initial frame, final frame and interpolation. More recently, Cyriaque Kouadio et al.[10] and Jose Daniel Ramos Wey et al.[7] built their real-time facial animation system based on a bank of pre-modeled 3D facial expressions. By the keyframe interpolation of predefined extreme expression, their system can produce a wide range of facial expressions. But the modeling of a complete bank of basic expressions can be quite time consuming, and all these basic expressions occupy space. The intermediate expressions are limited by the type of interpolation, and if two expressions do not blend nicely, more intermediate expressions must be added to the sequence. Furthermore, a complete bank must be built for any new facial model.

Parke[16] introduced the concept of parameterization in facial animation to address the disadvantages of the keyframe technique. Two parameter sets were built to control facial shape and facial expression respectively. The technique requires only a single face model, eliminating the need for a complete bank of models. The Facial Animation System developed by Steve DiPaola[2] is an extension of Parke's model whose purpose is to provide an environment for the easy creation, manipulation, and animation of face. It has the ability to specify and animate a wider range of facial types. The key aspect in these parameterized conformal and expression controls relies upon the parameterization itself. Too few parameters will offer only a limited spectrum of expressions, while too many parameters will overwhelm the animator creating a specific expression on a specific face. Thus, to develop a parameterization flexible enough to create any possible face, and allowing it to take any desired expression with simple and intuitive controls, is a very complex task.

Magnenat-Thalmann et al.[21] defined a model where the action of a muscle is simulated by a procedure, called an Abstract Muscle Action procedure(AMA). Each AMA has an associated procedure with a set of parameters which can be used to control the motion of vertices composing the face. Kalra et al.[8] describe interactive techniques for simulating facial muscle actions using Rational Freeform Deformation (RFFD). This method consists of deforming the predefined skin with a space-filling function whose purpose is to deform the skin surface corresponding to desired muscle actions. Hai Tao and Thomas S. Huang[19] propose a mesh-independent free-form deformation model. In their model, the connected piece-wise 3D Bézier volumes are generated automatically from a given face mesh according to facial feature points. These volumes cover most regions of a face that can be deformed. The facial animation model of Williams[25] is based on the tracking of the reflective markers on a performance actor. After recording, the displacements of markers are applied onto the 3D facial model. The deformation area around each marker is interpolated, leading to a library of realistic expressions.

Waters[23] presented a facial animation technique which modeled the effects of muscle tensions over a region of skin. While successful in the application, the model was purely geometrical rather than dynamic. It did not respond in a physically realistic fashion to external forces. For facial animation to be flexible and realistic, the force that is generated by facial muscle contraction must be modeled.

The purely geometric nature of prior face models mentioned above limits their realism, however, because it does not take into account the fact that the human face is not only a geometric model but also an elaborate biomechanical system. Physically-based face models have emerged to overcome these limitations. Platt and Badler[17] developed an early physical face model. In their model, skin is the outermost level represented by a set of 3D points defining a surface which is movable. Bones represent innermost level which cannot be moved. Muscles are groups of elastic arcs between the two levels. Essa et al.[4] employed the physically-based face model for observing and tracking facial motion using video sequences as input. Using Platt's model as the base model, they extended it to incorporate a multi-grid finite element mesh to describe the skin surface and developed an elastic model for the face muscles. Their muscle model

is a simplification of the model presented in [6], which consists of series and parallel elastic spring to generate muscle force. The important limitation of their method is the lack of "real" oris muscles. This limitation has resulted in unrealistic motion around the lips. Terzopoulos et al.[20] produced realistic facial animation using a hierarchical physical face model. They also estimated the contraction of facial muscles from facial image sequence. Their methods although very realistic, lack the speed to be able to run in real-time because of the underlying complexity of the calculations involved for each facial movement. Lee et al.[12] produced realistic facial animation using a hierarchical physical model of a human face. By exploiting high-resolution laser scanner data, the structured generic facial mesh can be conformed to individual automatically. However, his model only has one kind of facial muscle, which limits the scope of expression animation. For motion, it employs explicit Euler integration method. Rolf Koch et al.[9] presented an approach for surgical planning and prediction of facial shape by using finite element models. Although the system can achieve high performance, however, a quantitative analysis of the relationship between facial muscles and facial skin deformation has not been done in detail. And the high computation cost prevents its usage in real-time applications.

1.2. Preview

Our paper is organized as follows: first, we give an overview of our facial expression animation system and describe different processing components. Section 3 briefly introduces the FACS(Facial Action Coding System) which maps the desired facial expression into facial muscle activation. In section 4 we elaborate the modeling process of physical muscle models and motion of jaw. Section 5 presents anatomy-based multilayered facial tissue model for simulating the deformable nature of facial skin. The assembly process that enables the anatomically consistent facial skin to be constructed automatically is also described. Section 6 illustrates the motion dynamics and numerical simulation of our facial model. We finish by presenting our simulation results, some conclusions and future work.

2. System Overview

Our real-time facial expression animation system, illustrated in Fig. 1, consists of three parts: physical facial skin modeling, facial muscles definition and editing and mass-spring system solver.

In the first step, a multilayered face tissue model is built by using triangular wire meshes. The model represents the face tissue of three layers: epidermis, dermis and hypodermis. All vertices are connected by non-linear springs that represent the elasticity of facial skin.

The facial muscles definition process allows the user to interactively define the origin and insertion points of the facial

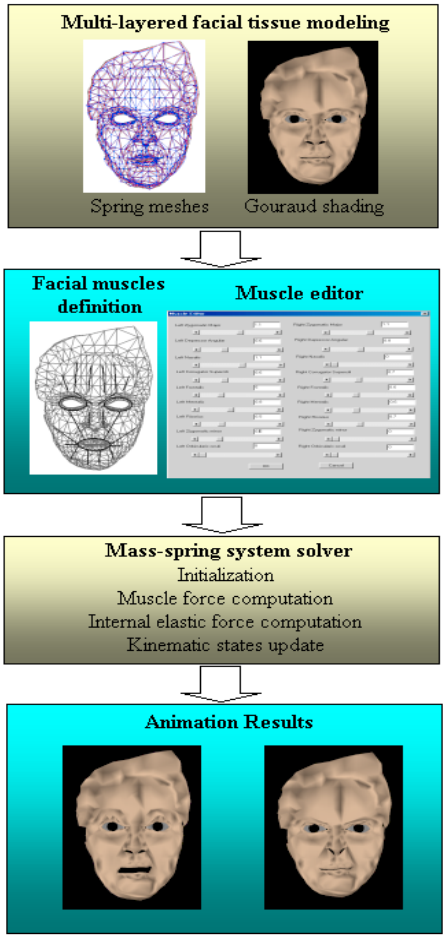

Figure 1: *System set-up for facial expression animation*

muscles. Muscle editor provides the interface for adjusting the value of muscle force scaling factor which determines the magnitude of the contraction of individual facial muscle. The user can combine a weighted sum of muscle contractions into Action Unit (AU) during muscle editing.

The mass-spring system solver computes the facial appearance of each Action Unit in order to obtain displacement fields for the face model. It comprises computations for individual muscle force, internal elastic force, updating kinematic states to obtain new face shape. By the appropriate combination of several AUs, the realistic expressions can be synthesized.

3. The Facial Action Coding System (FACS)

The simulation of facial expressions requires a mapping of the desired facial expression into facial muscle activation. The Facial Action Coding System (FACS) was developed by Ekman and Friesen [3] for this purpose. Based on photographs

AU No.	FACS Name	AU No.	FACS Name
AU1	Inner brow raiser	AU14	Dimpler
AU2	Outer brow raiser	AU15	Lip corner depressor
AU4	Brow lower	AU16	Lower lip depressor
AU5	Upper lid raiser	AU17	Chin raiser
AU6	Cheek raiser	AU20	Lip strecher
AU7	Lid tighter	AU23	Lip tighter
AU9	Nose wrinkler	AU25	Lip part
AU10	Upper lid raiser	AU26	Jaw drops
AU12	Lid corner puller		

Table 1: *Action Units employed*

of facial expressions, they investigated in fundamental psychological tests the relationship between facial expressions and emotions. The result of this research is a unique categorization of the emotions (happiness, fear, sadness, anger, surprise, and disgust) into primary facial expressions.

The FACS describes the set of all possible basic action units (AUs) performable by the human face. Each AU is minimal facial action that cannot be divided into smaller actions. There are 66 AUs in the FACS which are categorized as follows:

i. AUs of the upper face

ii. AUs of the lower face

1) Horizontal Action Units

2) Vertical Action Units

3) Diagonal Action Units

4) Orbital Action Units

iii. Mixed AUs

iv. Head and eye position

The groups (i) and (ii) play a major role in the simulation of facial expressions. We select 17 units which give strong influence to emotion expression. Table 1 shows the 17 AUs which we are actually using out of AUs to make expressions.

4. Facial Muscle Modeling

4.1. Facial Muscle Physiology

The muscles of the face are commonly known as the muscles of facial expression. Some facial muscles also perform other important functions, such as moving the cheeks and lips during mastication and speech, or constriction and dilation of the eyelids. The muscles of facial expression are superficial, they are mostly attached with both the skull and the facial tissue. A special case are obicularis oculi around the eyes and obicularis oris around the mouth which are only grown together with the tissue. One end of the facial muscle attached to skull is generally considered the origin while the other one is the insertion. Normally, the origin is the fixed point, and the insertion is where the facial muscle performs its action. The muscles of facial expression work synergistically and not independently. The group functions as a well-organized and coordinated team, each number having specified functions, one of which is primary. These muscles interweave with one another. It is difficult to separate the boundaries between the various muscles.

Muscles are bundles of muscle fibers working in unison. The shape of the fiber bundle determines the muscle type and its functionality. In human face, a wide range of muscle types exist: rectangular, triangular, sheet, linear, sphincter [24]. There are three main types of facial muscles incorporated in the face model:

- **Linear muscle:** It consists of a bundle of fibers that share a common emergence point in bone and pulls in an angular direction. One of the examples is the zygomaticus major which attaches to and raises the corner of the mouth.
- **Sphincter muscle:** It consists of fibers that loop around facial orifices and can draw towards a virtual center; an example is the orbicularis oris, which circles the mouth and can pout the lips.
- **Sheet muscle:** It is a broad, flat sheet of muscle fiber strands without a localized emergency point. The most obvious example is the lateral frontalis, one of the forehead muscles that raise the outer portion of the eyebrows.

4.2. Linear Muscle Model

On contraction, facial regions close to the skin insertion point of a muscle are affected. The effect of facial muscle contraction is to pull the surface from the area of the muscle insertion point to the muscle attachment point. Fig. 2 illustrates the linear muscle model with the following definitions:

$\mathbf{x}_i$: arbitrary facial skin point

m_j^A : attachment point of linear muscle j at the skull

m_j^I : insertion point of linear muscle j at the facial skin

R_j: the maximal radius of muscle influence

φ_j : the maximal angle of muscle influence

φ_{ji}: the angle between vector $m_j^A m_j^I$ and $\mathbf{x}_i$

l_{ji} : the distance between muscle attachment point m_j^A and skin point $\mathbf{x}_i$

The muscular influence decreases with both the decreasing of the distance from muscle attached point l_{ji} and increasing of the angle from muscle vector φ_{ji} . It is assumed

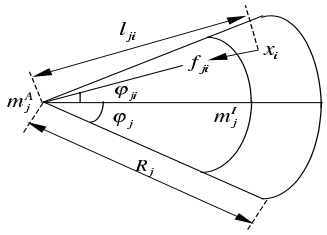

Figure 2: *Linear muscle model*

that there is zero influence at the point of muscle attachment to the bone m_j^A and that maximum influence occurs at the muscle insertion point m_j^I. Consequently, a fall-off of the muscle force is dissipated through the adjoining tissue in the influence area of the muscle. l_{ji} is calculated as:

$$l_{ji} = \|m_j^A - \mathbf{x}_i\| \tag{1}$$

l_{ji} and φ_{ji} are the weight factors that influence muscle j at vertex x_i separately for length factor λ_{ji} and angular factor γ_{ji} :

$$\lambda_{ji} = \frac{l_{ji}}{\|m_j^A - m_j^I\|} \tag{2}$$

$$\gamma_{ji} = \frac{\varphi_{ji}}{\varphi_j} \tag{3}$$

λ_{ji} defines the longitudinal distance of vertex i to muscle j normalized to values between 0 and 1. A value around 0, or 1 signifies that vertex i lies close to the muscle attachment point, or close to the insertion point, respectively. The influence of the muscle j increase with λ_{ji}. γ_{ji} is defined in [0,1] and represents the latitude distance between vertex i and muscle j. Increasing γ_{ji} results in decreasing the influence of muscle j. The muscular force applying at vertex x_i can be computed as:

$$\overrightarrow{f_{ji}} = \alpha_L \Theta_1(\lambda_{ji})\Theta_2(\gamma_{ji})\nu_{ji} \tag{4}$$

where

$$\nu_{ji} = \frac{m_j^A - \mathbf{x}_i}{\|m_j^A - \mathbf{x}_i\|} \tag{5}$$

In the equation(4), α_L is muscular force scaling factor which provides us the macro control of the magnitude of the muscle force. Function Θ_1(Fig. 3 (a)) scales the muscle force according to the length ratio, while Θ_2 (Fig. 3 (b)) scales the muscle force according to the angular ratio γ_{ji} at node $\mathbf{x}_i$. We define

$$\delta_j = \frac{R_j}{\|m_j^A - m_j^I\|} \tag{6}$$

and

$$\Theta_1(\lambda_{ji}) = \begin{cases} \cos((1-\lambda_{ji}^{\eta_j})\cdot\frac{\pi}{2}) & 0 \le \lambda_{ji} \le 1 \\ \cos((\frac{\lambda_{ji}^{\eta_j}-1}{\delta_j^{\eta_j}-1})\cdot\frac{\pi}{2}) & 1 < \lambda_{ji} \le \delta_j \end{cases} \tag{7}$$

$$\Theta_2(\gamma_{ji}) = \cos(\varphi_j\gamma_{ji})\cos(\gamma_{ji}\cdot\frac{\pi}{2}) \quad 0 \le \gamma_{ji} \le 1 \tag{8}$$

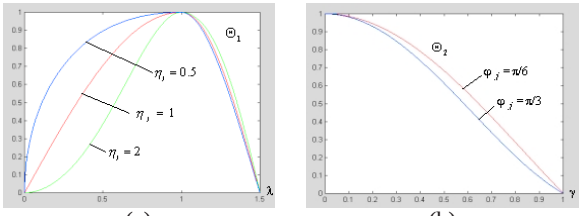

(a) (b)

Figure 3: *(a)Function curve of Θ_1 and the influence of parameter η_j; (b)Function curve of Θ_2 and the influence of parameter φ_j*

The constant η_j defines the muscle strength factor which provides us the micro control of the magnitude of the muscle force. A decrease in the value of η_j increases the muscle influence along the longitude.

4.3. Sphincter Muscle Model

Unlike the linear muscle, the sphincter muscle attaches to skin both at the origin and at the insertion, and contracts around a virtual center. Because sphincter muscles do not behave in a regular fashion, it can be modeled in elliptical shape and can be simplified to a parametric ellipsoid as shown in Fig. 4. The definition of the parameters are:

$\mathbf{x}_i$: arbitrary facial skin point

o: epicenter of sphincter muscle influence area

a: the semimajor axis of sphincter muscle influence area

b: the semiminor axis of sphincter muscle influence area

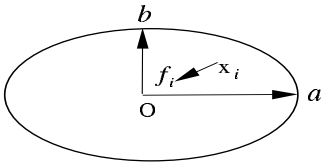

Figure 4: *Sphincter muscle model*

The muscular force applied at vertex x_i is computed as:

$$\overrightarrow{f_i} = \alpha_s \Theta(r_i)\nu_i \tag{9}$$

where α_s is sphincter muscular force scaling factor and

$$\nu_i = \frac{o - \mathbf{x}_i}{\|o - \mathbf{x}_i\|} \tag{10}$$

$$\Theta(r_i) = \cos((1 - r_i) \cdot \frac{\pi}{2}) \quad 0 \le r_i \le 1 \tag{11}$$

in equation (11)

$$r_i = \frac{\sqrt{y_i^2 a^2 + x_i^2 b^2}}{ab} \tag{12}$$

4.4. Sheet Muscle Model

A sheet muscle neither emanates from a point source, nor contracts to a localized node. In fact, sheet muscle is a series of almost-parallel fibers spread over an rectangle area, muscle model is illustrated in the Fig. 5. Two points m_j^{A1} and m_j^{A2} specify the attachment line of the sheet muscle. m_j^{Ac} is the middle point of $m_j^{A1}$and m_j^{A2} . Similarly, the points m_j^{I1} and m_j^{I2}specify the insertion line of the sheet muscle, and m_j^{Ic} is the middle point of m_j^{I1} and m_j^{I2}.

$\mathbf{x}_i$: arbitrary facial skin point

m_j^{A1} and m_j^{A2} : attachment points defining attachment line of sheet muscle j

m_j^{Ac}: middle point of sheet muscle attachment line

m_j^{I1} and m_j^{I2}: insertion points defining insertion line of sheet muscle j

m_j^{Ic} : middle point of sheet muscle insertion line

L_j : the length of the rectangle zone influenced by sheet muscle

W_j : the width of the rectangle zone influenced by sheet muscle

l_{ji} : the distance between skin point $\mathbf{x}_i$ and sheet muscle attachment line

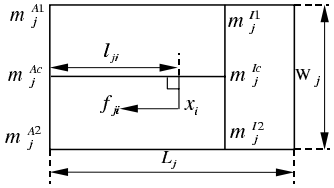

Figure 5: *Sheet muscle model*

In the sheet muscle model, the muscular force applied at vertex x_i is calculated as:

$$\overrightarrow{f_{ji}} = \alpha_{st} \Theta(\lambda_{ji}) m_j \tag{13}$$

where α_{st} is sheet muscular force scaling factor and

$$m_j = \frac{m_j^{Ac} - m_j^{Ic}}{\|m_j^{Ac} - m_j^{Ic}\|} \tag{14}$$

$$\Theta(\lambda_{ji}) = \begin{cases} \cos((1 - \lambda_{ji}^{\eta_j}) \cdot \frac{\pi}{2}) & 0 \le \lambda_{ji} \le 1 \\ \cos((\frac{\lambda_{ji}^{\eta_j} - 1}{\delta_j^{\eta_j} - 1}) \cdot \frac{\pi}{2}) & 1 < \lambda_{ji} \le \delta_j \end{cases} \tag{15}$$

in the formula (15), η_j is the sheet muscle strength factor and

$$\lambda_{ji} = \frac{l_{ji}}{\|m_j^{Ac} - m_j^{Ic}\|} \tag{16}$$

$$\delta_j = \frac{L_j}{\|m_j^{Ac} - m_j^{Ic}\|} \tag{17}$$

4.5. Jaw Rotation

In facial modeling and animation, it is very important to rotate jaw, which makes the animation convincing. Human jaw is composed of two parts: upper and lower jaw. The movable part is the lower jaw. In our model, the jaw contains the vertices of the lower region of the face surface which can rotate around the X and Y axes. The rotation of the jaw can be realized by a coordinate transformation as the following equation:

$$\begin{pmatrix} x_i' \\ y_i' \\ z_i' \end{pmatrix} = \begin{pmatrix} \cos\phi_y & -\sin\phi_x \sin\phi_y & -\cos\phi_x \sin\phi_y \\ 0 & \cos\phi_x & -\sin\phi_x \\ \sin\phi_y & \sin\phi_x \cos\phi_y & \cos\phi_x \cos\phi_y \end{pmatrix} \begin{pmatrix} x_i \\ y_i \\ z_i \end{pmatrix} \tag{18}$$

ϕ_x and ϕ_y represent the degrees of rotation around the X and Y axes respectively. The origin of the transformation are both sides of the joint points of the jaw and the upper skull.

5. Multilayered Facial Tissue Modeling

5.1. Physiology of Skin Tissue

In order to account for individual tissue behavior which is varying with age, gender, and ethnic group, it is crucial to distinguish between different facial tissue types. Therefore the elastic properties of living tissue have to be well understood. There exist numerous ariticles and books describing the mechanical and functional properties of the different anatomical structures. The book written in 1993 by Y. Fung[5] is the most fundamental one. Facial skin consists of three layers: epidermis, dermis and hypodermis. The epidermis, the outermost tissue layer, is just 0.1mm thick and is supported by the underlying dermis layer. The dermis layer is much thicker (0.6mm to 3.5mm) and responsible for the elasticity of the skin. The underneath hypodermis layer contains the fatty tissue and only slightly affects the elasticity of the facial skin. Therefore, the facial soft tissue comprises various substances with different elastic properties, which can not be modeled separately.

Experimental results in [5] have shown that living biological tissue has a non-linear, viscoelastic stress-strain relationship as shown in Fig. 6. Under low stress, dermal tissue offers very low resistance to stretch, but under greater stress it resists stretch much more markedly. The history of strain affects the stress, which means that the stress-strain relations in the loading and unloading processes are different. Each branch of a specific cyclic process can be described by

a non-linear pseudo-elastic function. Since the difference is insignificant, we approximate the non-linear relationship by a biphasic curve illustrated in Fig. 6.

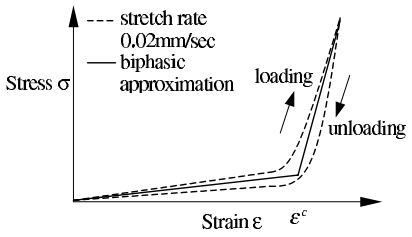

Figure 6: *Stress-strain relationship of facial tissue.*

5.2. Multilayered Deformable Tissue Model

In accordance with the structure of real skin, we have developed a multilayered mass-spring tissue model for facial expression animation. For each triangle of the facial skin one basic tissue element as shown in Fig.7 is created. Each mass point is linked to its neighbours by massless springs of natural length non equal to zero. The topmost surface of the lattice represents the epidermis. It is a rather stiff layer of keratin and collagen and the spring stiffness are set to make it moderately resistant to deformation. The springs in the second layer are highly deformable, reflecting the nature of dermal fatty tissue. Nodes on the bottom-most surface of the lattice represent the hypodermis to which facial muscle fibers are attached. Every vertex x_i^e in the surface mesh which represents the epidermis layer belongs to a vertex x_i^d on the underlying dermis layer and a vertex x_i^h on the hypodermis layer. This relation enables us to construct a mesh of springs between each two layers.

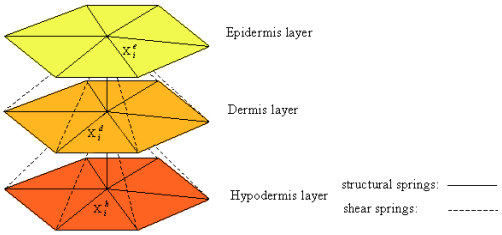

Figure 7: *Multilayered skin tissue element*

The basic tissue elements are generated by connecting each epidermis vertex to the underlying dermis and hypodermis structure. The linkage between each two layers is achieved in two different ways:

- Springs linking a vertex on each layer with its neighbors on the same mesh layer and springs linking this vertex with the corresponding vertex on the other layer, are referred to as structural springs, which resist compression or traction stresses. In particular the latter is normal to the connected layers.
- Springs linking a tissue layer vertex with the neighbors of the related underlying layer vertex, are referred to as shear springs, which resist shearing and twisting stresses.

The relationship of the springs is illustrated in Fig.7. By assembling the discrete deformable model according to histological knowledge of skin, we are able to construct an anatomically consistent facial skin surface. To automate the facial model assembly the procedure stars with the triangular facial mesh, whose mass points and springs represent epidermis. The point on the dermis layer x_i^d is computed by tracing the surface normal n_i^e of the epidermis in the direction to the dermis layer. n_i^e is approximated by averaging the normals of all adjacent triangles. The obtained discrete dermal nodes are interconnected by dermal springs to establish dermal layer which has the same topology as that of the epidemal layer. Then it forms intermediate spring mesh by attaching short springs from arbitrary epidermal node x_i^e downward to corresponding dermal layer node x_i^d and its neighbors. In the same way, the hypoepidermis layer can be constructed automatically.

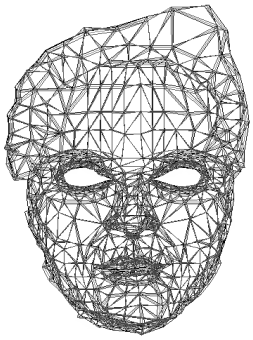

Figure 8: *Layered facial skin model*

Fig. 8 illustrates a facial topology after the automatic assembly. The synthetic tissue include about 1280 triangular elements. The spring meshes in the three layers which represent epidermis, dermis and hypodermis layer have different stiffness parameters in accordance with the nonhomogenecity of real facial tissue. To approximate the non-linear strain-stress relationship of the soft tissue each spring constant is defined biphasic(see Fig. 6). In order to simulate a homogeneous elasticity in each layer the spring constants depend not only on the flexibility of the actual individual tissue but also on the length of the springs and the size of the basic tissue elements, which is largely determined by the local curvature of the skin since there are large triangles in the regions of low curvature.

Tissue layer	Low spring stiffness (k_L)	High spring stiffness (k_H)
Epidermis	50	100
Dermis	20	40
Hypodermis	30	80

Table 2: *Spring stiffness parameters of different tissue layer*

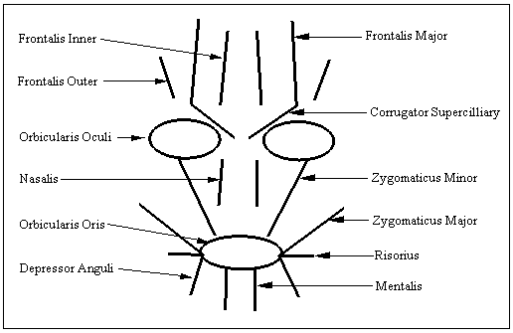

Figure 9: *Facial muscles in our model*

6. Forces and Dynamics of the Defomable Tissue Model

The internal elastic force is the resultant of the tensions of the springs linking $\mathbf{x}_i$ to its neighbours:

$$Q_i = -\sum_{j \in \mathcal{N}_i} k_{ij}[\mathbf{d}_{ij} - d^0_{ij}\frac{\mathbf{d}_{ij}}{\| \mathbf{d}_{ij} \|}] \tag{19}$$

where:

$\mathcal{N}$ is the set regrouping all neighboring mass points that are linked by springs to $\mathbf{x}_i$.

$\mathbf{d}_{ij} = \overrightarrow{\mathbf{x}_i\mathbf{x}_j}$.

d^0_{ij} is the natural length of the spring linking $\mathbf{x}_i$ and $\mathbf{x}_j$.

k_{ij} is the spring stiffness of the spring linking $\mathbf{x}_i$ and $\mathbf{x}_j$.

$$k_{ij} = \begin{cases} k_L & \varepsilon_{ij} \le \varepsilon^c \\ k_H & \varepsilon_{ij} > \varepsilon^c \end{cases} \tag{20}$$

The low-strain stiffness k_L is smaller than the high-strain stiffness k_H. Like real skin tissue, the biphasic spring is readily extendible at low strains, but exerts rapidly increasing restoring stresses after exceeding a strain threshold ε^c. Note that the spring force is a nonlinear function of node positions because $\| \mathbf{d}_{ij} \|$ involves roots of sums of squares. For all results presented in this paper we have assigned the stiffness values of Table 2 to the different tissue types.

Applying external forces to the deformable facial model yields realistic dynamics. Based on the FACS[3], various facial expressions are created by the combination of the contraction of certain facial muscles. In our 3D face model, there are 23 muscles. We use 3 sphincter muscles to represent the orbicularis oris and orbicularis oculi. The other muscles are represented as pairs of muscles which have left and right components. The facial muscle structure is shown in Fig. 9.

When the muscles contract, the facial skin points that are in the influence area of the muscle model are displaced to their new positions. As a result, the facial skin points not influenced by the muscle contraction are in an unstable state, and unbalanced elastic forces propagate through the mass-spring system to establish a new equilibrium state.

Based on the Lagrangian dynamics, the deformable facial model equations of motion can be expressed in 3D vector form by the second-order ordinary differential equation:

$$M\frac{\partial^2 \vec{\mathbf{x}}}{\partial t^2} + C\frac{\partial \vec{\mathbf{x}}}{\partial t} + K(\vec{\mathbf{x}})\vec{\mathbf{x}} = f(\vec{\mathbf{x}}) \tag{21}$$

We can take the elastic force expression as an external force $Q_k(\vec{\mathbf{x}}) = K(\vec{\mathbf{x}})\vec{\mathbf{x}}$, and take Q_k to the right hand side of the Eq. 21. This new form of the equation will simplify the formulation procedure.

$$M\frac{\partial^2 \vec{\mathbf{x}}}{\partial t^2} + C\frac{\partial \vec{\mathbf{x}}}{\partial t} = f(\vec{\mathbf{x}}) - Q_k(\vec{\mathbf{x}}) \tag{22}$$

in Eq. 22, $\vec{\mathbf{x}}$ is a 3n vector of nodal displacement, M is the mass matrix, an $3n \times 3n$ diagonal matrix which contains masses of the nodes as diagonal elements, and C is the damping matrix, an $3n \times 3n$ diagonal matrix which contains dampers of the nodes as diagonal elements. f is a 3n vector of muscular force applied to each node. The solution of the nodal displacement, velocity and acceleration at time $t + \Delta t$ can be obtained by using numerical integration. In the simulation, we use a second-order Runge-Kutta method [18] to integrate ordinary differential equations. We have chosen this method because it is more accurate and stable than Euler's method while retaining an acceptable time of execution.

The algorithm is as follows:

1. Initialization:
   - Form face model mass matrix M and damping matrix C;
   - Calculate the initial displacement, velocity and acceleration: x^0, $\dot{x}^0$, $\ddot{x}^0$;
   - Store matrix value in memory.
2. Time loop:
   - Calculate the external muscular force vector f based on the muscle models;
   - Calculate the elastic force vector Q_k from elastic force equations;
   - Solve for acceleration at time $t + \Delta t$ based on the

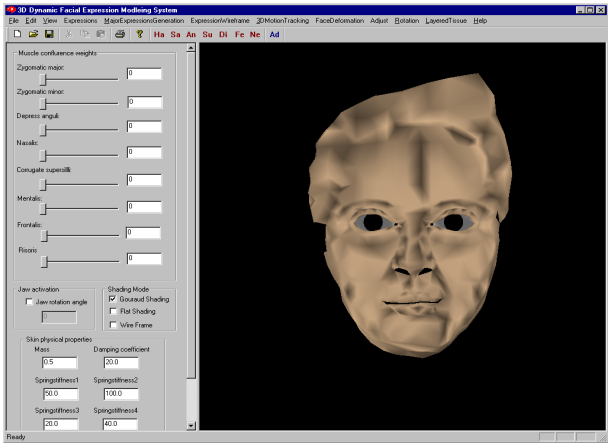

Figure 10: *Interface of the facial expression animation system*

stored matrix values(M,C), muscular force vector f and elastic force vector Q_k;

- Calculate new velocity and position at time $t + \Delta t$.

7. Results

We have implemented a facial expression animation system that illustrates how the physically-based multilayered tissue response to the muscle force to generate flexible expressions. The system is developed by C++/OpenGL. It runs on a SGI540 Visual Workstation, PIII-Xeon 550MHz, 512MB. Fig. 10 shows the graphical user interface to set the facial parameters, such as the combination weight of each facial muscle, the spring stiffness and damping coefficient of deformable tissue layers, and the rotation angel of the jaw. By the control panel, we can interactively adjust the values of parameters to produce various facial expressions.

In the simulation, we used the physically-based face model to create some typical facial expressions. They are sadness, anger, happiness, surprise and disgust. In each expression simulation, we select the major functional muscles based on the AUs of the FACS. For instance, sadness is represented by AU1+AU15 in the FACS, the associated facial muscles are frontalis and depressor anguli. By simulating the contraction of these facial muscles, the expression of sadness is regenerated dynamically. Fig. 11 shows the dynamic deformation of face model on “Anger" and “Surprise".

In Fig. 12, from left to right, the first images are the typical expressions produced by a real man for comparison. The second images show the expressions synthesized by the smoothly shaded facial model. The images on the right are the 3D motion tracking of the mesh nodes of the outmost tissue layer on the face model, which correspond to each synthesized facial expression respectively. In the motion tracking, the motionless vertices are in blue and the colorful trajectories illustrate the motion of the displaced vertices during expression generation process from blue at the first frame to red at the last frame. Note that all the synthesized expressions illustrated are generated dynamically. Regarding the system performance, we have reached the animation of 22 frames per second.

8. Conclusion and Future Work

In this paper, we have presented a 3D face model which is physically-based and constructed from anatomical perspective for facial expression animation. Three kinds of muscle models are developed to simulate real facial muscle contraction. The spring meshes that approximate epidermis, dermis and hypodermis have different mechanical parameters to simulate the nonlinear elastic behavior of the skin. Two types of biphasic nonlinear springs, structural springs and shear springs, are included in our model. Based on the Lagrangian dynamics, facial tissue is deformed as the muscle force applying on it. Experimental results show the real-time face deformation process as well as realistic expression animation. Using our facial model, we can generate flexible and realistic expressions.The biggest advantage of our expression modeling system is that it can analyze the relationship between the facial skin deformation and the inside state, which is determined by facial muscle parameters. This enables us to predict deformation of the facial shape by detailed quantitative analysis of the relationship between facial muscles and facial skin deformation.

For the future work, the skull model will also be included to accurately simulate the articulation of the chin which due to the movement of jaw. Texture mapping will be implemented to increase realism of animation. In order to account for individual variation of the different layers and tissue types, we will incorporate input data of the real skin from CT or MRI source. Moreover, we will research the relationship between facial expressions and the internal facial structure (muscle and skull) in addition to creating realistic facial images.

References

1. M. Cohen and D. Massaro, “Modeling coarticulation in synthetic visual speech," *Models and Techniques in Computer Animations*, pages 141-155, Springer-Verlag, Tokyo, 1993. 1

2. S. DiPaola, “Extending the range of facial types," *Journal of Visualization and Computer Animation*, 2(4): 129-131, 1991. 1, 2

3. P. Ekman and W. V. Friesen, *Facial Action Coding System* ,Consulting Psychologists Press Inc., 577 College Avenue, Palo Alto, California 94306, 1978.

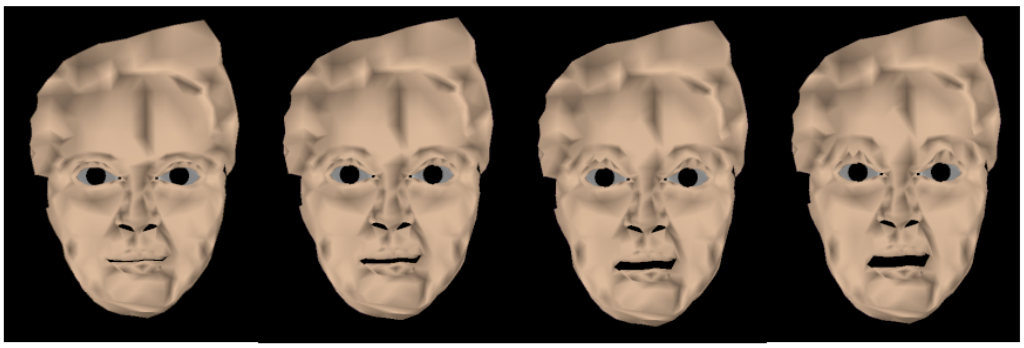

Neutral ————> Anger

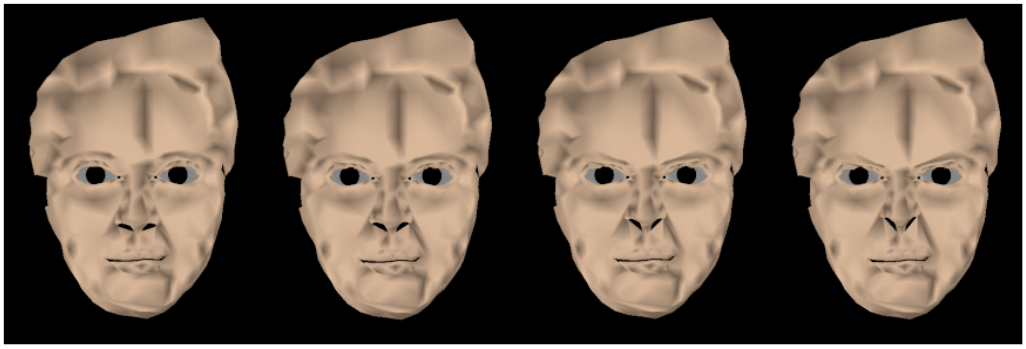

Neutral ————> Surprise

Figure 11: *Dynamic deformation of the face in expression of "Anger" and "Surprise"*

4. Essa, I. and S. Basu. "Modeling, Tracking and Interactive Animation of Facial Expressions and Head Movements using Input from Video", *Proceedings of Computer Animation 1996 Conference*, Geneva, Switzerland, June 1996.
5. Y. Fung, *Biomechanics: Mechanical Properties of Living Tissues*, Springer Verlag, New York, NY, 1993.
6. C. Ghez, "Muscles: Effectors of the motor systems," *Principles of Neural Science*, shapter 36, pages 548-563. Elsevier Science Publishing Co. Inc., third edition, 1991. 3, 8 1, 2 6 3
7. Jose Daniel Ramos Wey, Joao Antonio Zuffo, "InterFace:a real time animation system," *IEEE Proceedings of Computer Animation'98*, pages 41-48, 1998.
8. P. Kalra, A. Mangili, N. Magnenat-Thalmann, D. Thalmann, "Simulation of facial muscle actions based on rational free form deformatios," *Proc. EUROGRAPHICS'92*, pages 59-69. Cambridge, 1992.
9. Koch R., Gross M., Carls F., Buren D., Fankhauser G. and Parish Y., "Simulating facial surgery using finite element models," *Proc. SIGGRAPH'96*, vol.30, pages 421-428. ACM, August 1996.
10. Cyriaque Kouadio, Pierre Poulin, Pierre Lachapelle, "Real-time facial animation based upon a bank of 3D facial expression," *IEEE Proceedings of Computer Animation'98*, pages 128-136, 1998.
11. L. D. Landau and E. M. Lifshitz, *Theory of Elasticity* , Pergamon Press, London, UK, 1959.
12. Y. Lee, D. Terzopoulis, and K. Waters, "Realistic modeling for facial animation," *Proc. SIGGRAPH'95*, vol.29, pages 55-62. ACM, August 1995. 2 2 3 2 3
13. M. Nahas, H. Huitric, M. Saintours, "Animation of a B-Spline Fingure," *The Visual Computer*, **3**(5):272-276, March 1988.
14. Eben Ostby, *Pixar Animation Studios* , Personal communication, January 1997.
15. F. I. Parke, *Computer generated animation of faces*, Master's thesis, university of Utah, Salt Lake City, June 1972.
16. F. I. Parke, "Parameterized models for facial animation," *IEEE Computer Graphics and Application*, 2(9): 61-68, November 1982. 1 1 1, 2 1, 2

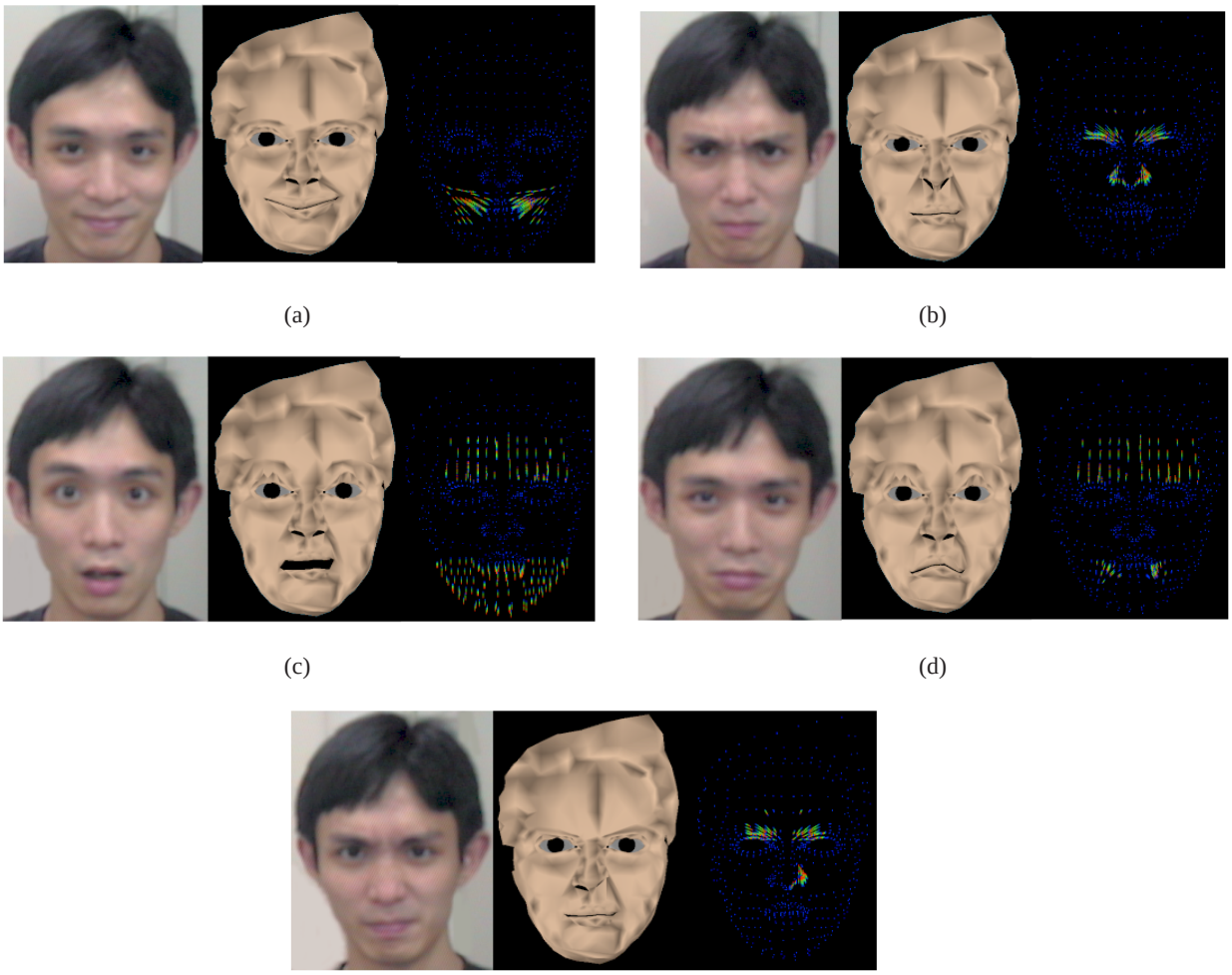

(a) (b) (c) (d) (e)

Figure 12: *Synthesized primary facial expressions (a)Happiness (b)Anger (c)Surprise (d)Sadness (e)Disgust*

17. Platt S, Badler N, "Animating facial expressions," *Proc. SIGGRAPH'81*, vol.15, pages 245-252. ACM, 1981. 1, 2
18. W. H. Press, B. P. Fannery, S. A. Teukolsky, and W. T. Verrerling, *Numerical Recipes: The Art of Scientific Computing*,Cambridge University Press, Cambridge, UK, 1986.
19. Hai Tao and Thomas S. Huang, " Facial animation and video tracking," *CAPTECH'98*, pages 242-253, 1998. 8 2
20. D.Terzopoulus and K. Waters, "Analysis and synthesis of facial image sequences using physical and anatomical models," *IEEE Tran. Pattern Analysis and Machine Intelligence*, 15(6):569-579, June 1993.
21. N. Magnenat-Thalmann, E. Primeau, and D. Thalmann, "Abstract muscle action procedures for human face animation," *The Visual Computer*, 3(5):290-297, 1988.
22. C. L. -Y. Wang and D. R. Forsey, "Langwidere: a new facial animation system," *Proceedings of Computer Animation '94*, pages 59-68, 1994. 3 2 1
23. K.Waters, "A muscle model for animating three-dimensional facial expression," *Proc. SIGGRAPH'87*, vol.21, pages 17-24. ACM, July 1987. 2
24. P. L. Williams, R. Warwick, M. Dyson and L. H. Bannister, *Grey's Anatomy, 37th Edition*, Churchill Livingstone, London, 1989. 4
25. L. Williams, "Performance-driven facial animation," *Proc. SIGGRAPH'90*, vol.24, pages 235-242. ACM, August 1990. 2